Water Erosion in Tyre and Bint Jbeil Districts (Lebanon) Jibal al-Butum Area as an Example

Ali Khyami * Ali-Talal Haidar ** Hussein El Hage Hassan***

Abstract

The Southern Lebanon region is one of the most exposed Lebanese areas to water erosion. The problem has not been managed though it threatens soil quality and sustainable agricultural production. Erosion hazard maps are an essential tool for soil and land conservation measures. This study applies a qualitative model for mapping soil water erosion hazards, using GIS, in a semi-humid region, with a scarcity of rainfall data, and an intensive agricultural production. Five basic maps, each with a different number of classes, were first produced. These represent the slope, the rock infiltration, the soil erodibility, the vegetation cover, and the rainfall erosivity. These maps were later summed to obtain an erosion hazard map. The model indicates that a large area (34.4%) is subject to high erosion, especially in tobacco and legume (chickpeas, wheat …) growing areas. Indeed, by the time of heavy rainfall intensity (November to March), the legume has not grown any foliage and the tobacco was not yet planted, leaving the surface exposed. During the validation of the model using fieldwork, raindrops, sheet, rill, and gully erosions were observed. This validation qualitatively indicated that the model used is highly suitable (80%) for mapping soil erosion hazard under Lebanese natural conditions, and therefore useful to recommend protection measures by setting priorities for possible planning interventions.

* Lebanese University, Faculty of Letters and Human Sciences. ali_khyami@hotmail.com. Corresponding author.

** Department of Earth Sciences, Faculty of Arts and Sciences, AUB, Beirut, Lebanon.

*** Lebanese University, Faculty of Letters and Human Sciences. Research laboratory: CEDETE (EA 1210). hussein.el-hage-hassan@ul.edu.lb.

Keywords: Bint Jbeil, Erosion hazard, Geology, GIS, Gully erosion, Jibal al-Butum, Map, Qualitative model Raindrop erosion, Rainfall erosivity, Rill erosion, Rock infiltration, Sheet erosion, Soil erodibility, South Lebanon, Tyre, Water erosion.

Introduction

Soil erosion is a two-phase process consisting of the detachment of individual soil particles from the soil mass, and their transport by erosive agents such as running water and wind. When sufficient energy is no longer available to transport the particles, a third phase, deposition, occurs (Morgan, 2005).

Soil erosion by water is a serious geo-environmental problem causing land degradation in Mediterranean countries, including Lebanon (*e.g.*, Bou Kheir *et al*., 2006). The Eastern Mediterranean region, because of its aggressive climate (Traboulsi, 2012), is known for its sensitivity to erosion, particularly in mountainous areas. The areas more prone to soil erosion and degradation are those with steep slopes, poor vegetation, and barren agricultural land throughout the winter season.

Several erosion models exist: physical, analog, and digital (Gregory & Walling, 1973). The digital models in turn can be subdivided into empirical and physically-based. The most widely applied erosion model over large areas is the Universal Soil Loss Equation (USLE: Wischmeier and Smith, 1978), and its subsequent Revised Universal Soil Loss Equation (RUSLE: Renard *et al.*, 1997). It is a statistically calibrated model that combines erosion-controlling factors based on runoff plot data.

Several estimates of water erosion hazards are available for different Lebanese areas. FAO (1986) indicates that the erosion rates in the Lebanese mountains reach 50 – 70 ton's ha^{-1} $year^{-1}$. (Bou Kheir *et al*. 2006) estimated that 34.5% of the central Lebanon soil was affected by higher rates. El Hage Hassan *et al.* (2015) indicated that 36.4% of the Aaqoura mountainous area (Northeast Lebanon) suffers a high water erosion rate. Charbel and El Hage Hassan (2017) suggested that 49.1% of the Bkassine forest (Southern Lebanon) is also subject to a high water erosion rate.

Although the USLE approach yielded globally significant results in the classification of erosion ranges, these remain subject to discussion:

a. The model was originally designed only for small areas and relatively gentle slopes (< 20%).
b. The lack of accurate data required by the model in some countriessuch as: rain precipitation over a short time scale, soil erodibility, and vegetation coverage.
c. In Lebanon, even though the total annual rainfall intensity data is available together with that for its monthly distribution, there is a major gap in these data over shorter time scales. The original model of Wischmeier and Smith (1978) requires that the time scale for the rainfall intensity data be available about every 30 minutes. As this availability is rare, some models pretend to produce forecasts for short-time scales out of a monthly or an annual distribution (Meusburger *et al.*, 2012; Devatha *et al.*, 2015). This forecast was not used here . Therefore only one category was assigned to the erosivity given by the rainfall intensity data (see below).

A qualitative model for erosion was already applied to Lebanon (see El Hage Hassan *et al.*, 2015). This study applies the aforementioned model, together with the weighing of the erosion forms proposed by Morgan (2005) for validation. The model is originally based on the methodology developed by FAO and UNEP (FAO-UNEP, 1997) as part of an action plan for the Mediterranean. The validity of the modified model by El Hage Hassan *et al*. (2017) was tested to be 80%. The latter combines soil erodibility, rock infiltration, topographic slope, land use, with rainfall erosivity. The weights of the different factors using this modified method have been previously calibrated (Bou kheir *et al.*, 2001). unfortunately, there is a large subjectivity in the assessment of the erosivity category (class) in available models applied to different Lebanese areas. An arbitrary gradual increase in the erosivity class value every 250mm rainfall was adopted in this study.

The aim of this study is to assess land sensitivity for water erosion in an agricultural Mediterranean area through a qualitative model. Thematic mapping is used to delimitate areas according to their potential hazard of erosion.

Study Area

The study area is located in the southeast part of the Tyre city, on the western edge of the Jabal Amel plateau, between 33° 07' E - 33° 12' N, and 35° 15' - 35° 21' E. It includes four villages: Zebqine, Jibal al-Butum, Yater, and Siddiqine. The area is mostly administratively governed by Tyre, except for the Yater town, which is located in the Bint Jbeil administrative

area. It has an overall surface of 4017.4. Hectares (42.6 km², max of 7.5 x 9.5 km). It is about 100 km away from the capital Beirut, and 20 km from Tyre (Fig. 1).

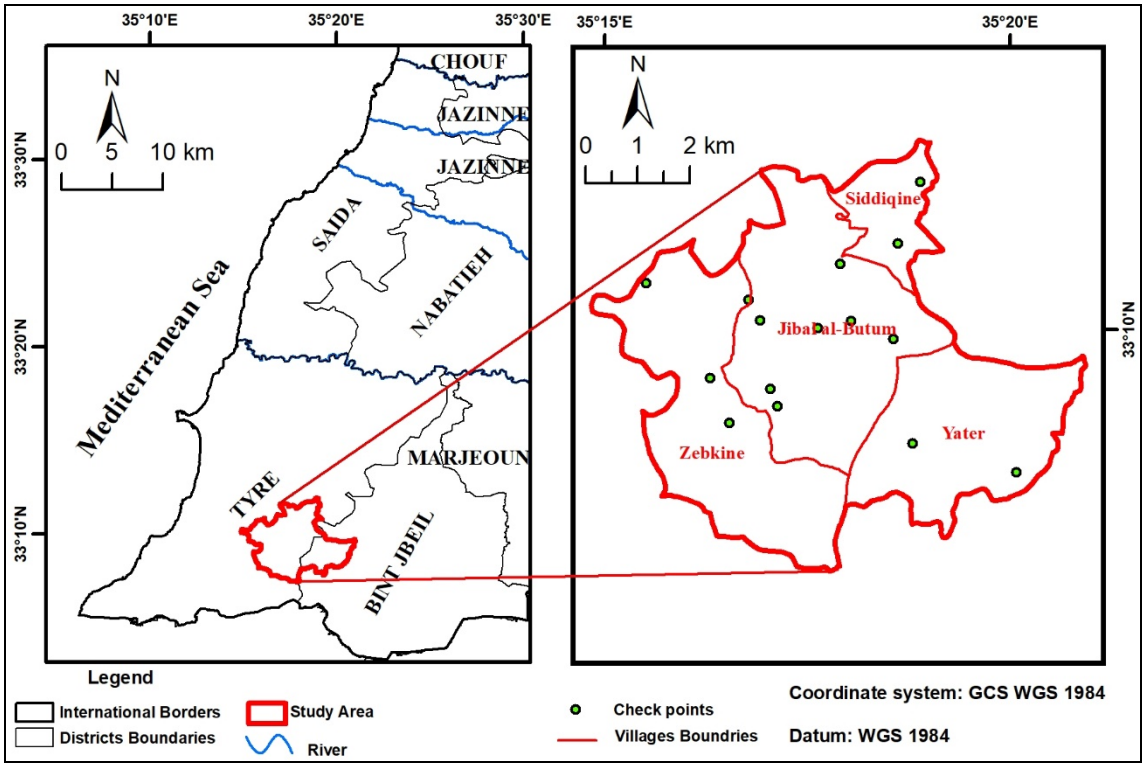

Figure 1. Location of the study area. The dots represent the validation point of the model on the ground. See text for details.

This agricultural (mainly tobacco) area was chosen as a model for Mediterranean soil with a relatively high erosion rate, as the soil remains bare during the rainfall season. It is also affected by a high topographic elevation to the east (700 m), and a maritime climate setting (the sea is at 5.5 km) to the west. This region is characterized by a semi-humid climate, with an average temperature of 18°C, and 700 mm rainfall annually most of which occurs in high-intensity storms between November and April.

The diversity of the Mediterranean vegetation is affected by several factors, including elevation from the sea, soil moisture, and solar radiation. The slopes of more than 20 degrees dominate (min 0.3 and max 73.5). The average elevation is 474 m (min 160 and max 758). The geology of the region is dominated by marly limestones and dolomitic limestones formations of mid and Upper Cretaceous, and mid-Eocene age.

The main economic activity is agriculture, especially tobacco and olive cultivation. Over the past two decades, deforestation led to large environmental degradation. Large swaths of forested

areas were converted to grow tobacco, leaving the soil vulnerable to erosion, especially during the intense rainy season. Tobacco cultivation extends in three stages. The first is the cultivation of tobacco nurseries in January over small areas. During this period, heavy rainfalls occur and the remaining large areas of bare land are directly subject to rainwater erosion. During the second stage, which begins in March, the grown tobacco seedlings are extracted and then cultivated in these remaining areas. The third stage begins in early June when tobacco is harvested in large areas.

Erosion occurs in the study area in several forms (Fig. 2). The most visible occur in the form of raindrops, sheet erosion, and rill erosion in many locations. In these areas, sheet and rill erosion were caused by high rainfall intensity storms in combination with limited infiltration of water into the soil, generating Hortonian overland flow (see *e.g.*, Davie, 2008). Several large permanent erosion gullies were also present, as a result of heavy rainfall and the absence of vegetation cover. They range in width from 1 to 5 m, and with a depth of > 1 m.

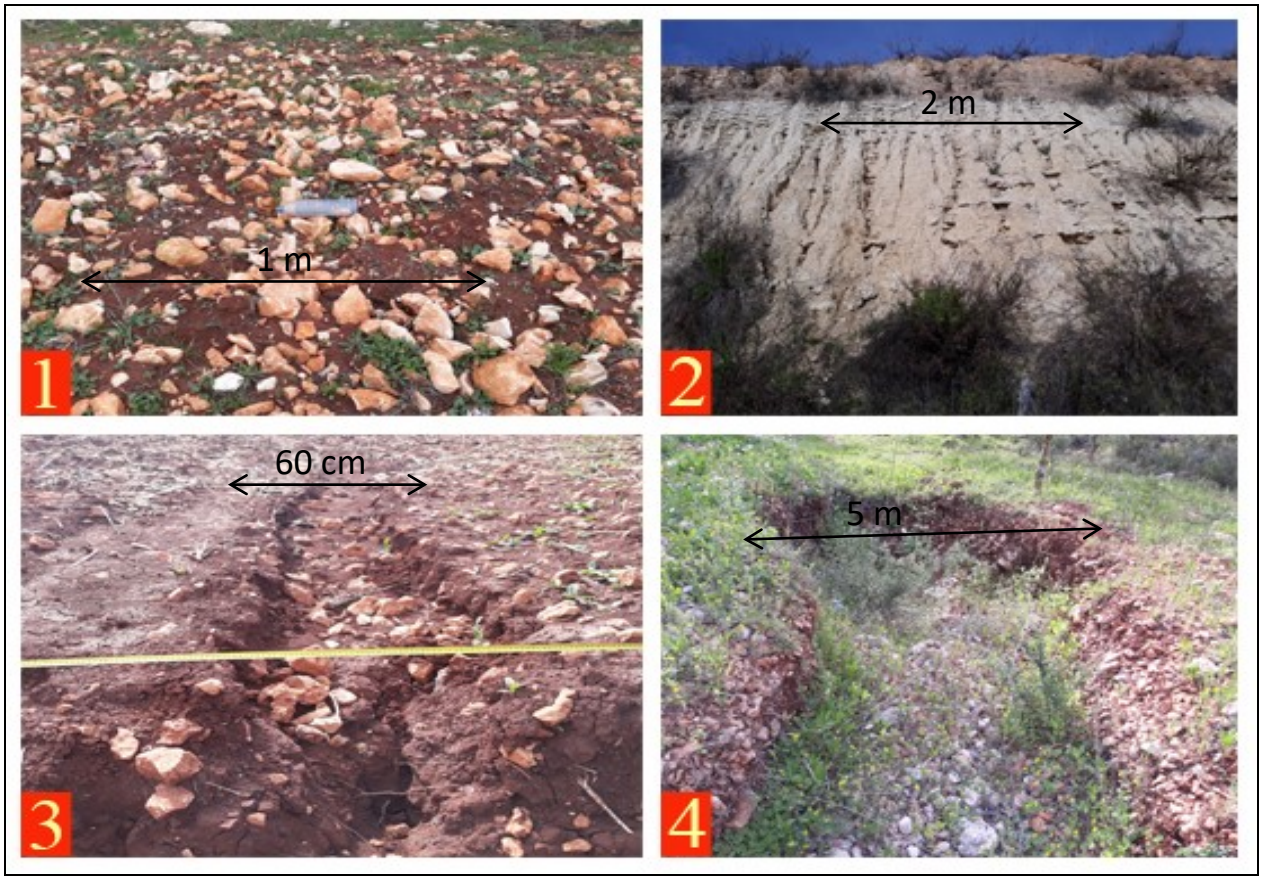

Figure 2. Forms of water erosion in the study area. 1) Raindrops Erosion, 2) Sheet Erosion, 3) Rill Erosion, and 4) Gully Erosion.

Materials and Methods

For each factor affecting soil erosion (soil erodibility, rock infiltration, rainfall erosivity, slope factor, and vegetation cover), a class value was assigned: very low = 1, low = 2, moderate = 3, high = 4, and very high = 5 (see El Hage Hassan, 2011; Charbel & El Hage Hassan, 2017; El Hage Hassan, 2019).

The erosion hazard map was qualitatively generated using the expert system type, by overlapping the 5 types of thematic maps. Due to the scarcity of rainfall data, the rainfall erosivity was included as being uniform (only 1 class). Based on the weighing of coefficients given by Charbel and El Hage Hassan (2017), a value of 0.19% was applied to indices attributed to soil erodibility, rock infiltration, topographic slope, and erosivity of rainfall (Fig. 3). Assuming a strong role of vegetation as protection against water erosion, a higher coefficient for vegetation cover (0.24%) was retained.

The resulting assessment of the overall erosion hazard will be monitored using values from 1 to 5.

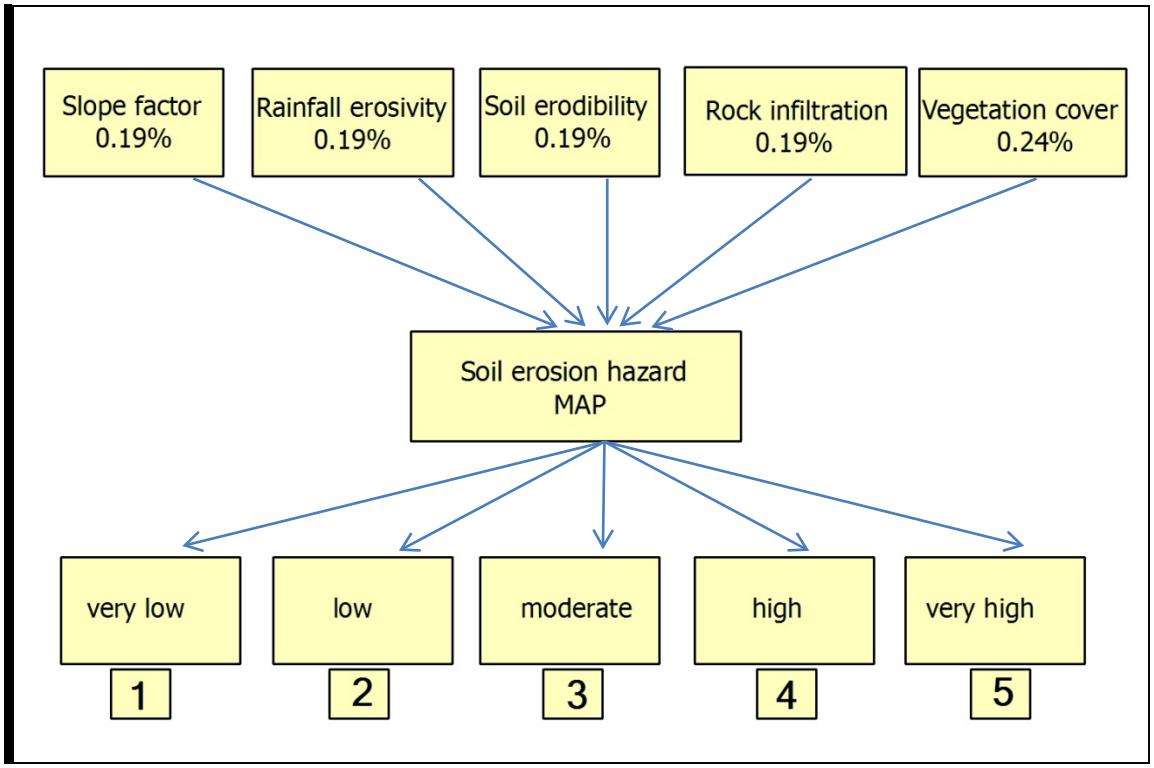

Figure 3. The hierarchy of the qualitative model applied to produce the soil hazard classes. (See text for details).

In the presented maps, there was a use of the Lambert Conformal Conic projection. To show the maps in a 3D perspective, the hillshade format raster was overlapping the other maps, and then the contrast decreased.

To apply the qualitative model, the following maps and data were used:

a. The six different types of soil present in the study area and the thickness of the soil cover were both identified using the soil map of Naqoura - Bint Jbel - Lebanon (Darwish *et al.* 2006) at the scale of 1/50,000.
b. The reported values for soil grain size analyses, and organic matter content, accompanying the soil map of Lebanon of Darwish *et al.* (2005) rely on only a few samples, and these were not collected from the area of the present study. The texture and the organic matter content of six soil samples (one for each soil type) were collected at a depth of 20 cm and were investigated at the Laboratory of Scientific and Agricultural Research Department (LARI), Al-Fanar, Lebanon.
c. The topographic map of Tyre – Nabatieh (Lebanon)at the scale of 1/20,000 (contour equidistance 10 m) was published in a raster format by the Directorate of Geographical Affairs of the Lebanese Army (DAGG), then it was geo-referenced. The contours were redrawn and the slope therefore generated.
d. Sentinel-2 satellite image with a spatial resolution of 10 m wasacquired in January 2020 It was used to determine the land use types.
e. Rainfall data from the Climate Atlas of Lebanon (MTPT, 1977) were used to calculate the rainfall erosivity.
f. The geological map of Aita el Chaab, Jouaia, and Nakoura, at the scale of 1/20,000, (Guerre, 1973) were used to determine the geologic formations, and consequently the rate of infiltration (see Bou Kheir, 2001).

The Elements of the Model

Soil erodibility

The resistance of soil to erosion is a function of its structure, moisture, roughness, organic matter content, *etc*. (Dwivedi, 2018). The susceptibility of soil to erosion agents is generally referred to as soil erodibility (Lal, 2001). Overall, the weight of the soil erodibility factor is set in the present model (see above) to 19%. When this value is taken to 100%, then the texture was

assigned a partial weight of 40%, organic matter content for another 40%, and depth for the remaining 20%. Overall and partial soil and erodibility weights are based on El Hage Hassan *et al*. (2016).

Soil unit names are given in Darwish *et al*. (2006) for the whole Lebanese territory (soil map of Lebanon, 1/ 50.000). They claim to have used the soil classification system of the World Reference Base for soil information (WRB, 1998). Accordingly, they have identified six soil types (Table. 1) in the study area. In the present study, one sample was analyzed for texture and organic content from each area covered by any soil type (Table 1). The results, together with the depth information, were used in the model.

Table 1. The first column represents the soil unit names. Columns 2 and 3 show the calculated area these units cover in this study. Five samples resulted as sandy clay loam (moderate sensitivity), whereas the last (Eutric Leptosols) as sandy loam (high sensitivity).

Soil Unit	Area (ha)	% Area	Sand %	Silt %	Clay %	OM %	Depth (cm)
Anthropic Regosols	21.7	0.5	67.2	15	17.6	2.2	100
Areno-Eutric Leptosols	2386	59.3	55.1	16.1	28.6	2	50
Calcaric Leptosols	135.9	3.3	58	14.3	27	1.4	45
Calcaric Regosols	26.9	0.6	54.5	15.2	30.2	4.6	60
Eutric Cambisols	37.8	0.9	55.4	15.9	28.6	1.2	130
Eutric Leptosols	1409.1	35	62.2	15.2	22.5	5.7	50

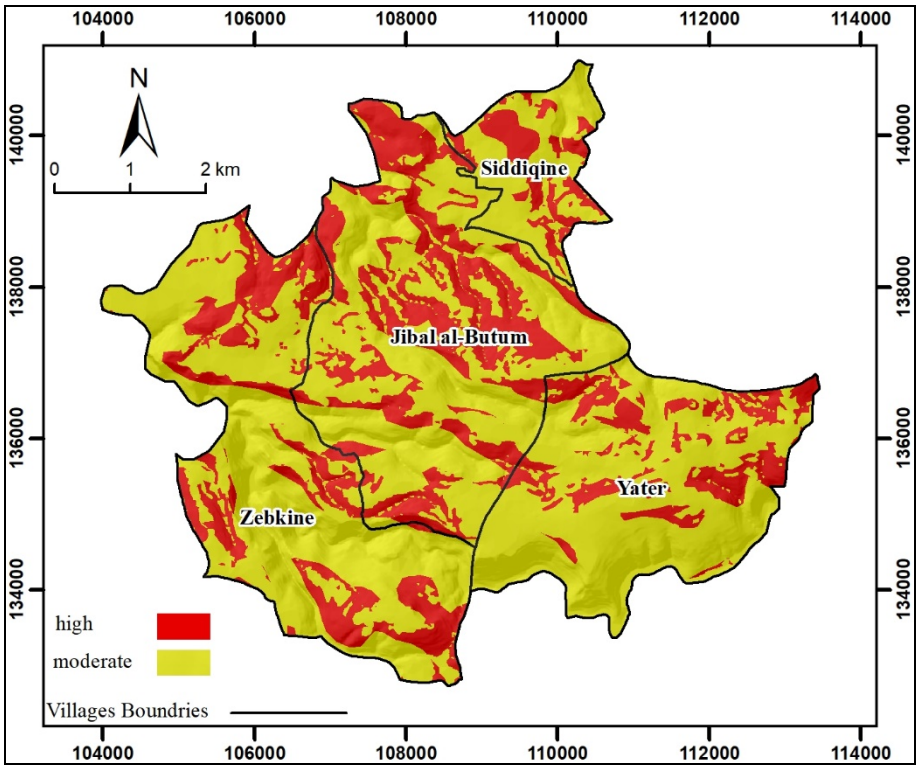

Figure 4. Soil erodibility map. The boundaries were derived by assessing the erodibility classes using Antoni *et al.* (2006) that were applied on the boundaries which were given by Darwish *et al.* (2006). (See text for details).

The erodibility class 3 (moderate) covers 69.7 % of the study area (2796.5 ha), and class 4 (high) 30.3 % (1218.4 ha).

Geologic Formations and Rock Infiltration

With respect to the lithologic description of the Lebanese geologic Formations, Walley revised the use of stratigraphic codes (1997) , while Nader *et al.* (2014). produced a generalized stratigraphic column subdivided into a northern and a southern part. For the south of Lebanon, the Formations present in the study area (Sannine, Maameltain, and Chekka) are represented by marly limestones for the Cenomanian, overlain by Turonian limestones, with a total thickness of 800 m. An unconformity spans over the Coniacian with parts of the Santonian. The upper part of the Santonian together with the Campanian and the Maastrichtian (600 m) are represented by shallow marine fossiliferous limestones. A second unconformity covers approximately the end of the Upper Cretaceous together with the Lower Paleocene. The Upper Paleocene and the lower

part of the Eocene are represented by shallow marine marly limestones overlain by reefal limestones with a total thickness of 150m+.

With the help of biostratigraphy, Dubertret (1951) attempted a geologic mapping of Lebanon with a chronostratigraphic aim (1/200000 for the whole of Lebanon, and 1/50000 sheets for the different areas). Guerre (1973) produced a minimum of 23 detailed (1/20000) geologic maps for some Lebanese areas, most of these cover southern parts of Lebanon. Fig. 5 includes an assembly of parts of 3 of these detailed maps.

The Sannine Formation ($C4_{a-b-c}$) is composed of a coastal and a mountainous member (Walley, 1997). Parts of the members ($C4_{b-c}$) of this mid-Cretaceous Formation are represented in the area (Fig. 5) mainly by shallow-water limestones. It occupies the smallest part (0.7%) as compared to the other Formations and is characterized by a medium rate of infiltration (Bou Kheir *et al.*, 2006) where most of the karstic springs occur in Lebanon (Dubertret, 1955).

The Maameltain Formation (C^{o}_{a-b}) is composed of white grey marls and marly limestones. This formation represents the largest part of the area (65.7%) and it is characterized by a medium rate of infiltration (Bou Kheir *et al.*, 2006).

The term Sannine - Maameltain Formation is used making no differentiation between the two Formations, given the large similarity in their physical properties in the area. It is composed of limestonesand marly limestones (area 27.2%) It is characterized by a medium rate of infiltration.

The Chekka Formation (C6) is composed of white and marly chalks, with phosphate and chert levels (area 4.8%). The Lutetian (mid-Eocene) (e2) is mainly composed of marly limestones (area 1.6%). Bou Kheir *et al.* (2006) estimated a very low infiltration rate for both formations.

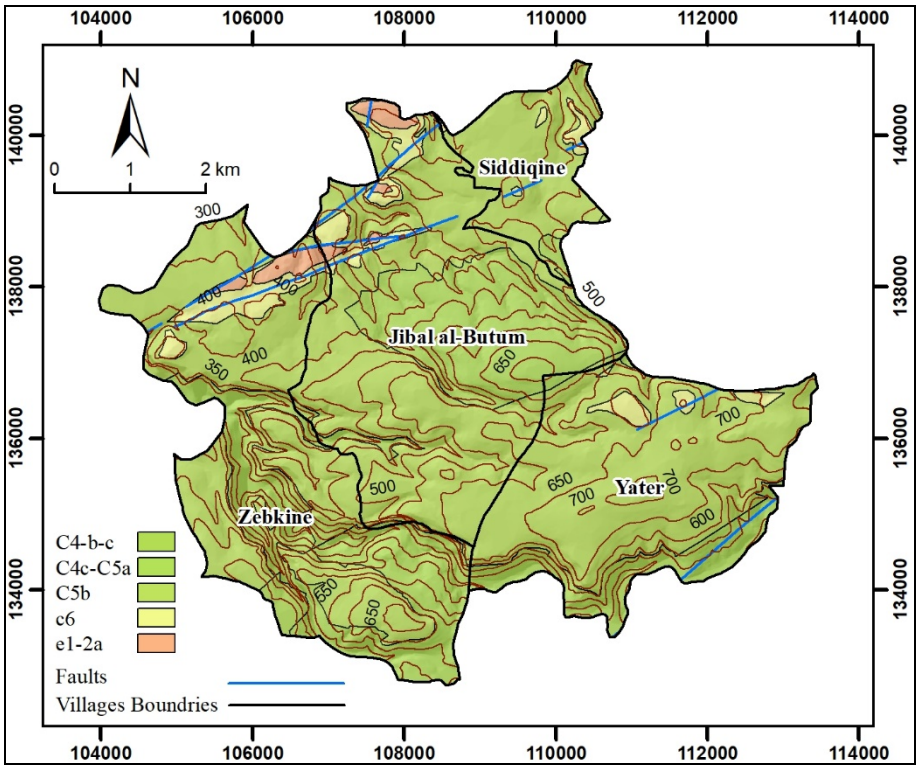

Figure 5. Geologic map of the study area from Guerre (1973), with the colors being updated using Gradstein *et al*. (2020).

Only two classes of rock infiltration were distinguished (Fig. 6). Moderate for C4, C5, and C4-C5 (infiltration class = 3) covering 93.6 % of the study area (3764.8 ha), and very low for C6 and e1-2a (class = 5) 6.4 % (252.5 ha).

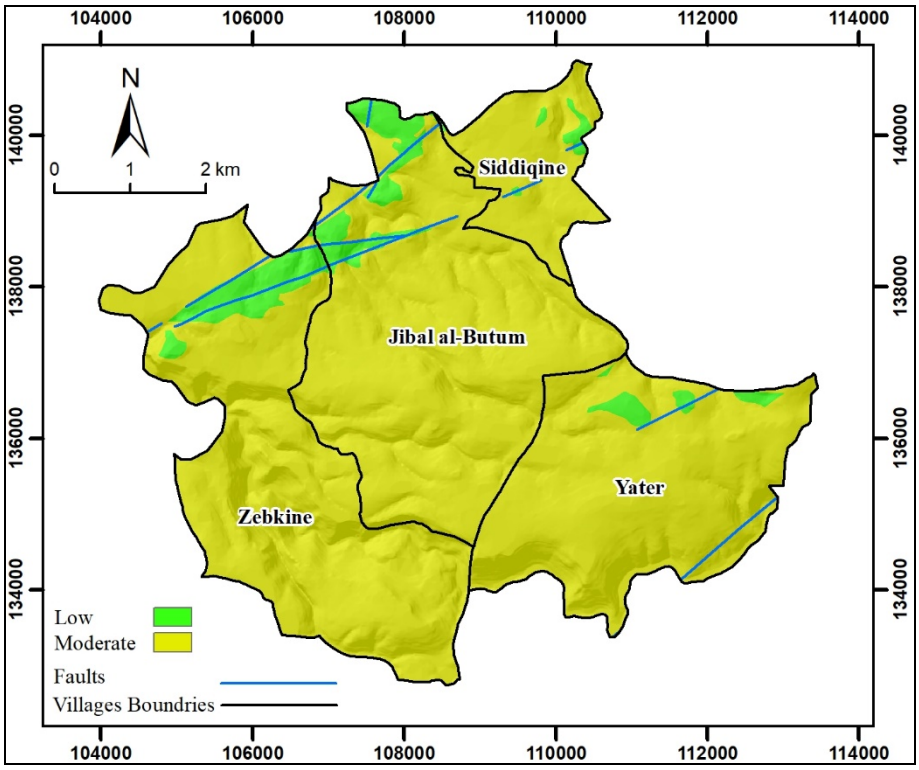

Figure 6. Rock infiltration that apply to the study area(Bou Kheir *et al.* ,2006).

Slope factor

Erosion would be expected to increase with increasing slope steepness as a result of the increase in velocity and volume of surface runoff. Furthermore, while on a flat surface raindrops splash soil particles randomly in all directions, on a sloping ground more soil is splashed downslope than upslope with the proportion of the splashed raindrops increasing as the slope steepens (Morgan, 2005).

Several studies in the Mediterranean area have selected the gradient of the slope (rise/run) as the only parameter representing the topographic index for erosion (see El Hage Hassan *et al.*, 2013 and references therein). The contour lines of the topographic map were used to produce the gradient map. Five classes (Fig. 7 and Table 2) were distinguished.

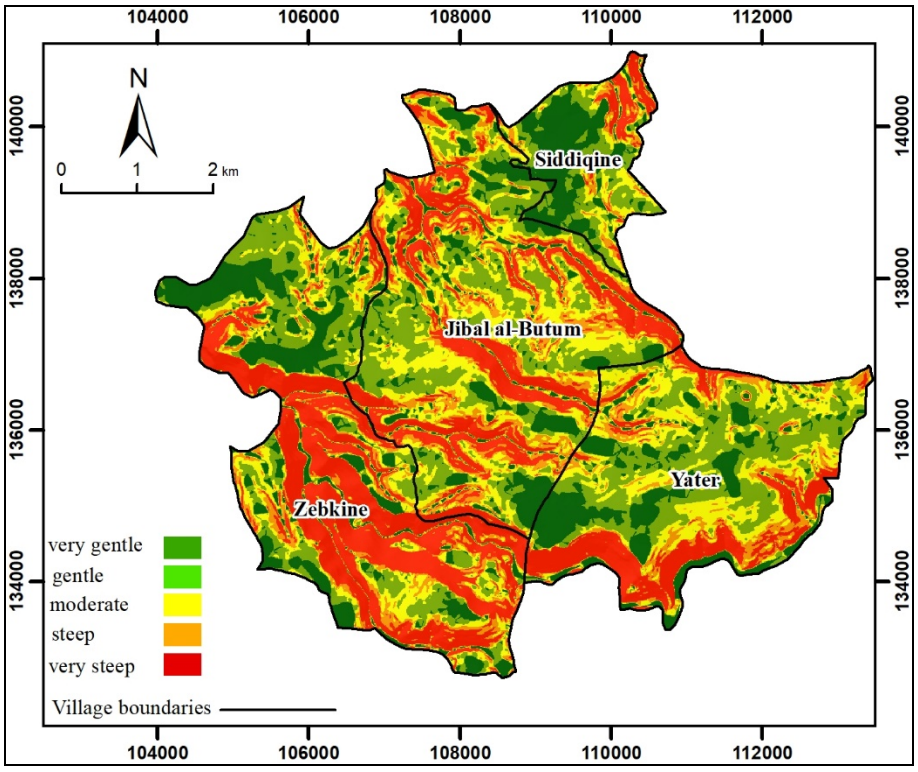

Figure 7. Slope factor map showing the gradient (see text for details).

Table 2. Slope factor class assignment based on slope gradient. The table shows also the area occupied by each slope gradient.

Gradient	Slope class	Slope	Area (hectare)	% Area
0°-5°	1	Very gentle	736.4	18.3
5°-10°	2	Gentle	989.9	24.6
10°-15°	3	Moderate	762.3	18.9
15°-20°	4	Steep	474.7	11.8
>20°	5	Very Steep	1054.1	26.2

Rainfall erosivity

The rainfall erosivity can be defined as an inherent capacity (energy) to initiate the soil erosion process (see *e.g.*, Blanco &Lal, 2008). The rainfall, by its intensity and energy, is the main determinant of the loss of soil. Morgan (2005) indicated that two rainfall types can introduce significant soil erosion when the short-lived intense storms exceed the infiltration capacity of the soil, and when the prolonged storms of low intensity saturate the soil.

The Eastern Mediterranean, including the Lebanese rainfall pattern, is apparently made of a mixture of these two types.

Table 3 compares some of the proposed models of soil water erosivity in Lebanon. It shows a large difference in the assignment of the index (class) corresponding to a given total annual rainfall. In this study, Bou Kheir *et al.* (2006) class assignment was followed where a new class is added every 250 mm rainfall. The average rainfall is based on monthly data from 2 meteorological stations located close to the investigated area. Since this average varies between 650 and 750 mm per year (MTPT, 1977), then only a class of 3 was assigned.

Table 3. Comparison of erosivity category (class) assignment in the available literature on Lebanese areas.

Annual Rainfall (mm)	Erosivity	Erosivity Class	Reference
0-250	very low	1	Bou Kheir *et al*. (2006)
250-500	low	2	
500-750	moderate	3	
750-1000	high	4	
>1000	very high	5	
1500	high	4	El Hage Hassan *et al*. (2015)
850-1000	N/A	3	Charbel and El Hage Hassan (2017)
1000-1250	N/A	4	

The vegetation cover (land use)

Vegetation acts as a protective layer or buffer between the atmosphere and the soil. The above-ground components such as leaves and stemsabsorb some of the energy of falling raindrops and running water, so that less is directed to the soil. While the below-ground components that comprise the root system affect the mechanical strength of the soil (Morgan, 2005).

The land and vegetation cover (Fig. 8) was assessed using the Sentinel-2 satellite image taken in 2020. Two kinds of image classification are widely applied, unsupervised and supervised. Unsupervised classification is used in the absence of prior knowledge of the study area. This process is based on the software analysis of the image without the user providing any training sites (Alrababah & Alhamad, 2006). Supervised classification is used when the user has prior

knowledge of the study area (field data, satellite images, aerial photographs), or when there is an ability to identify the types of land cover from the satellite image. Several algorithms are used in supervised classification: Maximum Likelihood classification, Minimum-Distance to the Mean Classifier, and Parallelepiped Classifier. Maximum likelihood classification is considered one of the best algorithms used in the classification processes (Thomas *et al*., 2015), and was chosen to mapping the land cover classes in the study area. In this method, the software is trained on a set of data collected from the training areas, then the program compares each known pixel (training sites) with unknown pixels, and then assigns unknown pixels to a specific category based on similarity or higher probability (Jensen, 2005; Kuzucu & Balcik, 2017). Based on field observations, five main classes were indexed (1 to 5) with 1 for the smallest effect on erosionand 5 for the largest (Table 4, Fig. 8).

Table 4. The proportion of the area with different land use.

land use	Vegetation Class	Area (hectare)	% Area
Dense vegetation (forest)	1	783.3	19.4
Scattered vegetation	2	422.1	10.5
Olive groves	3	692	17.2
Grasslands	4	1083	26.9
Tobacco and legumes	5	751.6	18.7
Urban areas	N/A	285.4	7.10

Only after the model has completely been computed, El Hage Hassan *et al* (2018) artificially assigned a class of “very low” to the water erosion hazard for urban areas. This is due to the relatively high stability of human settlement, although some parts of it may locally be subject to quite a high erosion rate with rills and gullies being formed at the sides of some roads. This assignment was adopted in this study.

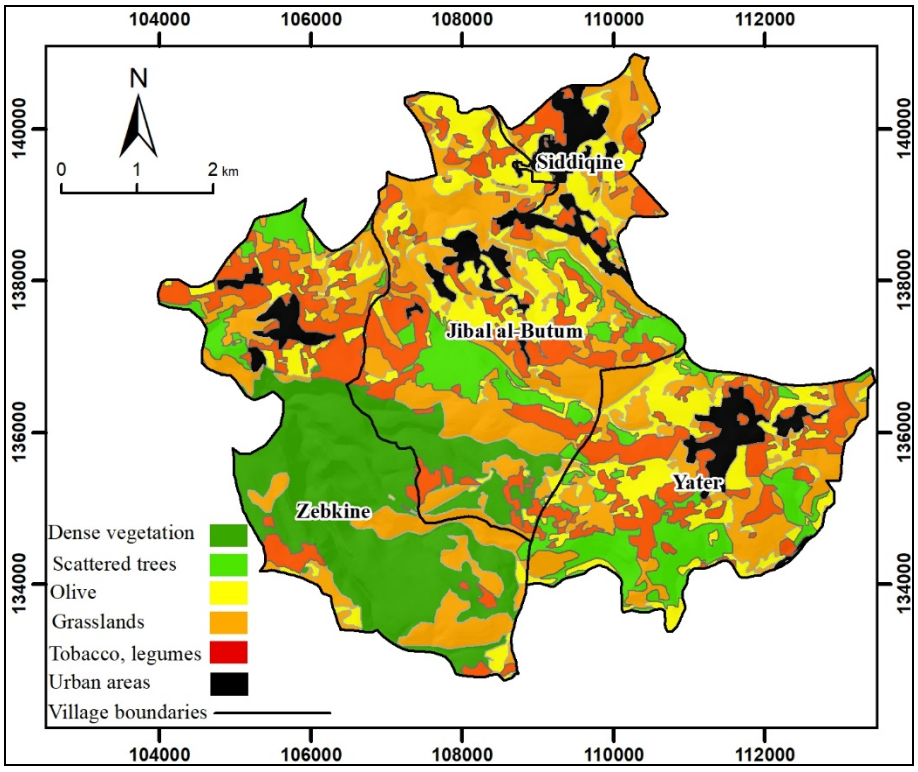

Figure 8. Land and vegetation cover using supervised classification.

The validation – fieldwork

The validation was performed by fieldwork. Each point (Fig. 1) is located at the center of a large surveyed area of about 200x200 m to 500x500 m.

Results

The model

The use of the qualitative model enabled the classification of the land according to its sensitivity to erosion, based on the integration of several thematic maps that were each related to a factor affecting water erosion. The resulting erosion hazard map included therefore 4 categories (Table 5 and Fig. 9):

Table 5. The proportion of the surface area of the different erosion hazard classes.

Erosion Hazard	Class	Area (hectare)	% Area
Very low (Urban area)	1	285.4	7.1
Low	2	104	2.5
Moderate	3	2241.4	55.8
High	4	1383.4	34.6

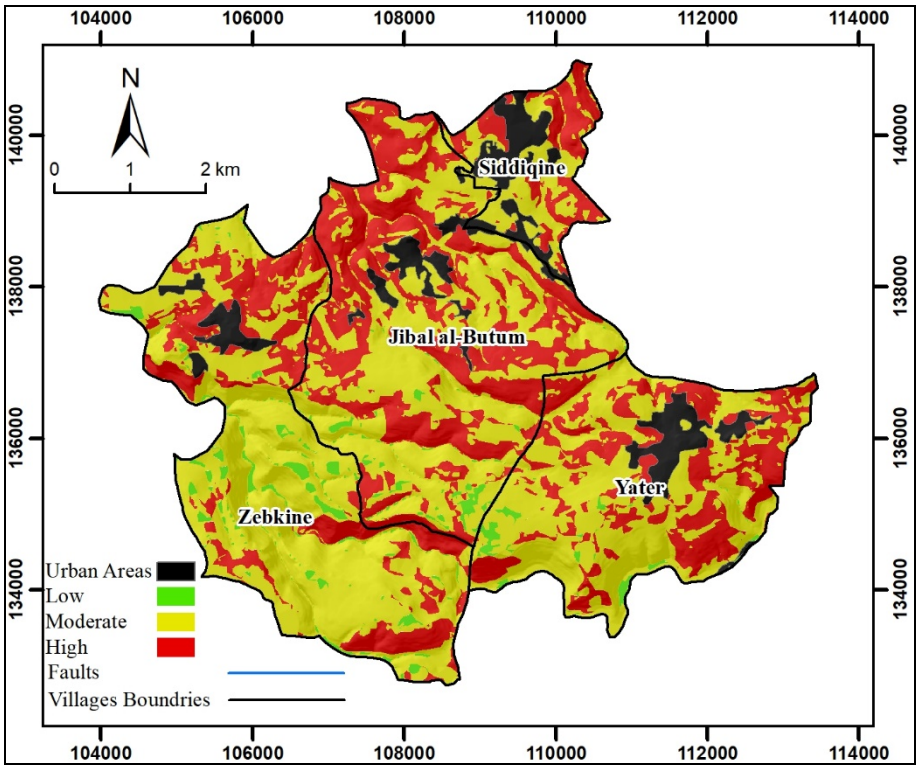

Figure 9. Soil erosion hazard map. Note the absence of "very high" erosion hazard classes in natural environments. Fig. 9 allows for the calculation of the proportion of the spatial distribution for each class of hazard and its relationship to each type of land use (see Table 7).

Table 7. Soil erosion percent area for the different land-use types.

Land-use Type	Total Area (he)	% Area Very Low Hazard	% Area Low Hazard	% Area Moderate Hazard	% Area High Hazard
Dense Vegetation	783.6	0	69.90	31.68	0.00
Scattered Trees	422.5	0	7.42	92.58	0
Olive trees	692	0	0	92.55	7.45
Grassland	1083	0	0	27.68	72.32
Tobacco and Legumes	285.4	0	0	26.85	73.15
Urban Area	751.8	100	0	0	0

These categories were selectively used to produce a map showing only high hazard areas (Fig. 10). This map shows the factor with the highest influence on water erosion for every single area .

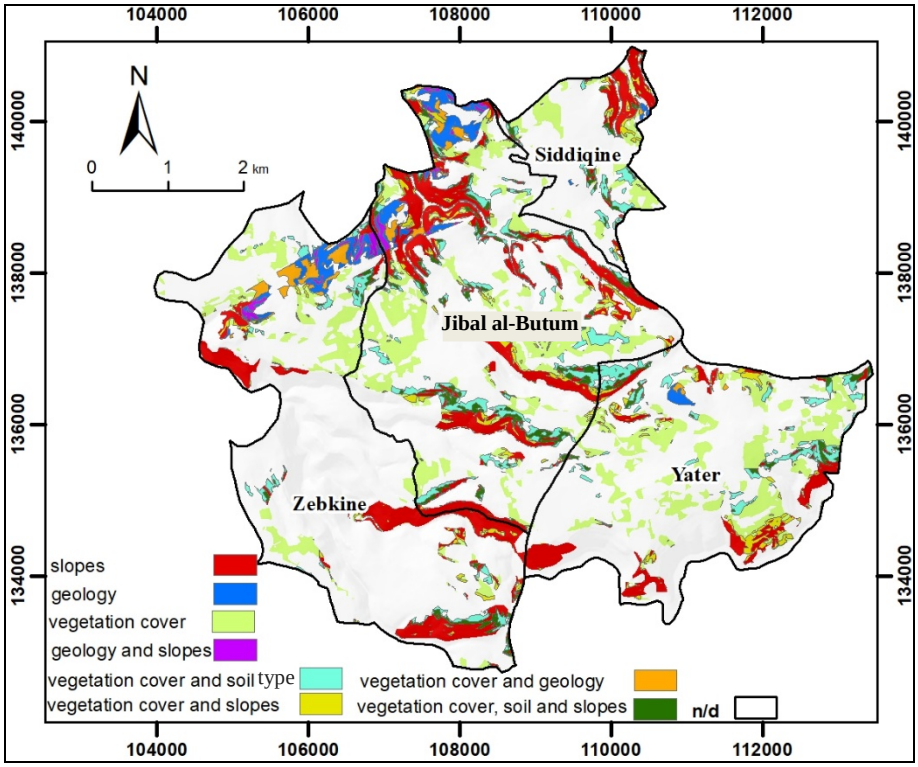

Fig 10. Map showing high erosion hazard areas classified according to the major factor influencing water erosion.

Fig. 10 was used to infer the relative proportion (see Fig. 11) of the area affected by a dominant factor leading to a high hazard water erosion over the whole area of study.

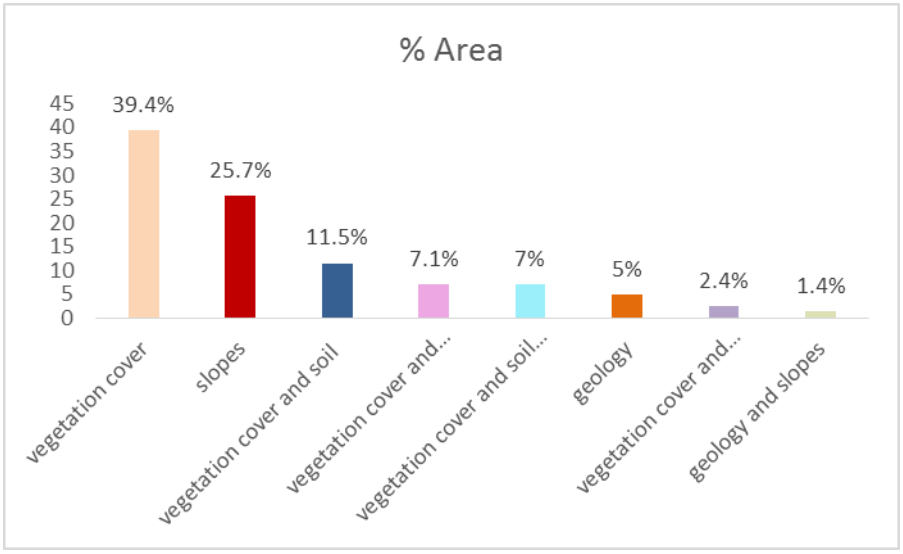

Fig 11. Histograms showing the area proportions for each factor responsible for the high hazard erosion. The data of this figure refer only to the areas indicated in Fig. 10.

Model Validation

Soil erosion

The validation (table 8) is based on the majority of the erosion forms observed within each area with gullies indicating a high hazard, rills moderate, and sheets low (see Morgan, 2005).

Table 8. Fieldwork validation for erosion. "False" indicates no matching of the model by validation. The coordinates show the validation location using the Lambert projection.

Land use	Validation	Justification of discrepancy	X	Y
Olive	False	Spacing between olive trees	108959	137516
Olive	True		109852	139005
Olive	True		108327	137384
Olive	True		110137	135180
Tobacco or legumes	True		105037	138239
Tobacco or legumes	True		106996	137920
Tobacco or legumes	True		107215	137537
Tobacco or legumes	True		108750	138609
Dense vegetation	True		106259	136425
Dense vegetation	True		107548	135890
Dense vegetation	True		106630	135568
Dense vegetation	False	Vegetation dispersed Locally	107409	136215
Grassland	False	Dense distribution of grass	110285	140180
Grassland	True		112136	134620
Grassland	True		109767	137176

Discrepancy justification

The common practice in Lebanon is to keep a linear distance d of about 5 m between any two planted olive trees. This distance leads to an assessed moderate erosion rate (Figs. 8 and 9). The erosion rate was assessed to be high where olive trees had a sparser distribution (d > 6 m),. Olive

trees are planted in terraced land which preserves the irrigation water and reduces the risk of erosion.

The erosion rate for the tobacco and legume areas was constantly high, producing rill and sheet erosions and gullies, independently of the agricultural spacing. The gullies were large (1 to 1.5 m width, and 1 to 1.2 m depth) and frequent (sometimes about once every 1 km^2).

In the dense vegetation area, the erosion rate was low except for only one location where a unique rill is present (moderate erosion rate) in a small area with locally sparse vegetation cover (line 12 of able 8).

A high erosion rate was observed in large parts of the grassland area except for few places where the grass cover was dense (thus having a moderate rate).

Mass Wasting

Only creep and debris flow/rock slide was observed, although they were not included in the model. Creep was observed in the areas of steep slopes with a vegetation cover, mainly with planted pine trees outside the forests. These trees had clearly curved trunks. Debris flow/rock slide was observed in areas having steep slopes without any tall vegetation cover. The weak zones that lead to this type of movement were, most of the time, surfaces that are perpendicular to the oxidized surface of the original rock. This original rock is massive, not showing clear bedding planes. The total area affected by both creep and debris flow is minimal, therefore not considerably affecting the model. The absence of cliffs also contributed to the reduction of the erosion rate.

Discussion and Conclusions

The qualitative model allowed for mapping the sensitivity of land to water erosion in four municipalities (Zebqine, Jibal al-Butum, Siddiqine, and Yater) in the south of Lebanon. The model is based on five factors, namely slope, vegetation cover, rainfall erosivity, soil erodibility, and rock infiltration. Each factor was assigned a weight estimating the degree of its sensitivity to erosion. The weighed factors were then added to obtain the final erosion hazard map.

The results indicate that the highest rates of erosion correspond to the legume and tobacco growing areas. Areas of grassland and clear-cut forests are affected by the highest erosion rates only when located on steep slopes. These highest erosion rate areas cover about the third of the

total investigated area. On the other hand, the low erosion rates correspond to the areas of mountains with dense vegetation cover.

The areas with the highest rates of hazard are concentrated in the North, with special distribution in the NW as compared to those with moderate hazard in the SW. Two major clusters of urban areas (very low erosion hazard) are located in the N-NW and the central E.

The fieldwork revealed several forms and intensities of erosion in the area of tobacco, olive growing areas, and bare soil. Several aspects of the model were confirmed. High erosion hazards were concentrated in the agricultural areas. Sheet erosion developed with an average of nearly 20 cm width, 20 cm depth, and 5 m length. Rill erosion was particularly concentrated on tobacco areas with an average of 60 cm width, 20 cm depth, and 10 m length; and gully erosion with 5 m width, 2 m depth and 10 m length.

Even though the currently used geologic map of Guerre (1973) differs to some extent from that of Dubertret (1951) for the study area, the effects of this difference on the results of the model turned out to be negligible. This however doesn't necessarily imply that the effects of such differences in the maps on erosion models would also be negligible in other areas.

The lowest hazard resulted in the areas with a dense vegetation cover and a very gentle slope. This is probably due to the reduction of the raindrop energy, the interception of the runoff, and the increase of the infiltration rate. Rills and gullies are present in agricultural areas and nearly absent in the forest.

Most of the results of the model were confirmed by the validation. In addition to the map with maximum hazard influence, samples of soil were tested for texture and organic content. The sand proportion was high in most of the samples. The source rock was assumed to contain a considerable proportion of sandstone, therefore leading to a relatively lower proportion of the organic matter in the soil.

Human activities accelerated erosion by changing the land use type especially by transforming the forest in the SW into tobacco growing areas, thus turning their sensitivity from low to high hazard.

The hazard distribution map helps planners and decision-makers to develop strategies and policies that should maintain soil stability and productivity. Afforestation is, therefore, necessary to reduce the erosion hazard, especially in grassland and tobacco growing areas.

An alternative type of agriculture is to be recommended that is both economically viable, and limits to a large extent the erosion hazard. A possible quick solution is to plant olive trees. Tobacco is only a short term solution.

Although the qualitative model seems to be effective in classifying the land according to its sensitivity to erosion, quantitative studies become more urgent to estimate the extent of soil losses. Also, a more extensive validation work is to be carried out reassessing the theoretical assignment of the classes used in the model. As an example, the area of tobacco and legumes was classified with a high erosion rate (only) although the large size of the gullies observed may indicate that this rate might be very high.

Fieldwork revealed that even a considerable addition of organic fertilizer unexpectedly did not protect the soil from high erosion rates during the heavy rainfall period (December to February), with the addition of organic material to the soil apparently not contributing decisively to its cohesion.

The present model could be considerably improved by testing many selected points for rock infiltration. Furthermore, the database of texture analyses, already performed on a selection of samples could be enhanced. Finally, a more elaborate model may take into account both soil erosion and mass wasting hazards, especially for areas where mass wasting covers a considerable proportion. This will provide the needed link between surficial (few cm to few m) and deeper (up to tens of m) movements.

Future studies may expand the database of tested soil samples, even for the whole surface of Lebanon. Rock infiltration was empirically not tested on any sample in the study area. This is a major subject for future research.

References

- Alrababah, M., & Alhamad, M., (2006). Land use/cover classification of arid and semi-arid Mediterranean landscapes using Landsat ETM. *International Journal of Remote Sensing*, Taylor & Francis, 27(13), pp. 2703-2718.
- Antoni, V., Le Bissonnais, Y., Thorette, J., Zaidi, N., Laroche, B., Barthes, S., Daroussin, J., & Arrouays, D., (2006). Modélisation de l'aléa érosif des sols en contexte Méditerranéen à l'aide d'un Référentiel Régional Pédologique au 1/250 000 et confrontation aux enjeux locaux. *Étude et Gestion des Sols*, 13, pp. 201-222.
- Bou kheir, R., Girard, M., Shaban, A., Khawlie, M., Faour, G., & Darwish, T., (2001). Apport de la télédétection pour la modélisation de l'érosion hydrique des sols dans la région côtière du Liban. *Télédétection*, 2(2), pp. 79-90.
- Bou kheir, R., Cerdan, O., & Abdallah, C., (2006). Regional soil erosion risk mapping in Lebanon, *Geomorphology*, 82, pp. 347-359.
- Blanco, H., & Lal, R. (2008). *Principles of Soil Conservation and Management*. Springer, 129 p.
- Charbel, L., & El Hage Hassan, H., (2017). Modélisation de la perte de sol dans la forêt de Bkassine (Liban sud), *Geo-Eco-Trop*, 41(31), pp. 479-492.
- Darwish, T., Khawlie, M., Jomaa, I., Aboudaher, M., Awad, M., Masri, T., Shaban, A., Faour, G., Bou kheir, R., Abdallah, C., & Haddad, T., (2006). *Soil map of Lebanon 1/50000*. CNRS-Lebanon, Monograph Series, 4, Liban, 367 p.
- Davie, T., (2008). *Fundamentals of Hydrology (2nd* ed*.)*. Routledge Taylor & Francis, 220 p.
- Devatha, C.P., Deshpande, V., & Renukaprasad, M.S., (2015). Estimation of Soil Loss Using USLE Model for Kulhan Watershed, Chattisgarh - A Case Study. *Aquatic Procedia*, 4, pp. 1429–1436.
- Dubertret, L., (1951). Carte géologique au 1/50000. Feuille de Naqoura- Bint Jbeil au 50000e. Ministère des Travaux Publics, Beyrouth, avec notice (sous la direction de L. Dubertret).
- Dwivedi, R., (2019). *Geospatial Technologies for Land Degradation Assessment and Management*. (1st ed.). CRC Press, 429 p.
- El Hage Hassan, H., 2011, Les Apports d'un SIG dans la connaissance des évolutions de l'occupation du sol et de la limitation du risque érosif dans la plaine de la Békaa (Liban). Exemple d'un secteur du Békaa el Gharbi. Orléans: Université d'Orléans, thèse de doctorat en géographie, 381 p

- El Hage Hassan, H., Touchart, L., & Faour, G., (2013). La sensibilité potentielle du sol à l'érosion hydrique dans l'ouest de la Bekaa au Liban. *M@ppemonde*, 109, 17 p.
- El Hage Hassan, H., Charbel, L., & Touchart, L., (2015). Cartographie des conditions de l'érosion hydrique des sols au Mont-Liban: exemple de la région d'El Aaqoûra, *Physio-Géo*, 9, pp. 141-156.
- El Hage Hassan, H., Charbel, L., & Touchart, L., (2018). Modélisation de l'érosion hydrique à l'échelle du bassin versant du Mhaydssé, Békaa-Liban, *Vertigo*, 18(1), 12 p.
- Cartographie de l'aléa érosif dans le bassin sud du Litani-Liban Hussein El Hage Hassan, Ghaleb Faour, Laurence Charbel et Laurent Touchart Rev. Int. Geomat., 29 (2), pp. 159-184.
- FAO, (1986). Conservation and management of soils in the countries under development. *Bulletin Pédologique*, 33, 98 p.
- FAO-UNEP, (1997). *Guidelines for mapping and measurement of rainfall-induced erosion processes in the Mediterranean coastal areas*. Priority Actions Programme, Regional Activity Centre (PAP/RAC), Split (Croatie), 72 p.
- Gregory, J., & Walling, E., (1973). *Drainage basin form and process*. Edward Arnold, 447 p.
- Guerre, A., (1973). Carte géologique au 1/20000, Aita el Chaab, Jouaya, and Nakoura.
- Hawie, N., (2014). *Architecture, Geodynamic Evolution and Sedimentary Filling of the Levant Basin: A 3D quantitative approach based on seismic data*. Thesis for the degree of Doctor of Philosophy, L'Université Pierre et Marie Curie, 250 p.
- Jensen, J., (2005). *Introductory Digital Image Processing. (3rd* ed.*)*, New York, Prentice Hall, 544 p.
- Kuzucu., A, & Balcik., F, (2017). Testing the potential of vegetation indices for land use/cover classification using high resolution data. *Remote Sensing and Spatial Information Sciences*, the International Society of Photogrammetry and Remote Sensing, IV-4 (W4), pp. 279-283.
- Lal, R., (2001). Soil degradation by erosion. *Land Degradation & Development*, 12(6), pp. 519-539.
- Meusburger, K., Steel, A., Panagos, P., Montanarella, L., & Alewell, C., (2012). Spatial and temporal variability of rainfall erosivity factor for Switzerland. *Hydrology and Earth System Sciences*, 16, pp. 167–177.
- Morgan, R.P.C., (2005). *Soil erosion and conservation* (3rd ed.). Oxford, UK. Blackwell, 316 p.

- MTPT, (1977). Atlas climatique du Liban. Tome 1: Pluie, température, pression, nébulosité. Édit. Ministère des Travaux Publics et des Transports, Service Météorologique, Beyrouth (Liban), 45 p. + planches (50 p.).
- Gradstein, F., Ogg, J., & Schmitz, M., & Ogg, G., (2020). *A Concise Geologic Time Scale* (2nd ed.)**.** Elsevier, 1300 p.
- Renard, K., Foster, G., Weesies, G., McCool, D., & Yoder, D., (1997). *Predicting soil erosion by water: a guide to conservation planning with the Revised Universal Soil Loss Equation*. Handbook, 703, 407 p.
- Thomas, L., Kiefer, R., & Chipman, J., (2015). *Remote Sensing and Image Interpretation (7th ed.)*. Wiley, 770 p.
- Traboulsi, M., (2012). La saison pluvieuse au Proche-Orient: une tendance au raccourcissement. *Climatologie*, 9, pp. 9-29.
- Wischmeier, W.H., & Smith, D., (1978). *Predicting rainfall erosion losses*. A guide to conservation planning. 282, 66 p.
- Walley, C., (1997). The Lithostratigraphy of Lebanon: A Review[1]*. Lebanese Science Bulletin*, 10, 20 p.
- World Reference Base for Soil Resources (1998). IUSS, ISRIC and FAO, Rome, 82.